



HAL
open science

Use of Sentinel-1 Time-Series for Archaeological Structures Detection

Florent Michenot, Giovanni Manfredi, Régis Guinvarc'H, Laetitia Thirion-Lefevre

► **To cite this version:**

Florent Michenot, Giovanni Manfredi, Régis Guinvarc'H, Laetitia Thirion-Lefevre. Use of Sentinel-1 Time-Series for Archaeological Structures Detection. IGARSS 2021 - 2021 IEEE International Geoscience and Remote Sensing Symposium, Jul 2021, Brussels, Belgium. pp.5183-5186, 10.1109/IGARSS47720.2021.9555144 . hal-03616691

HAL Id: hal-03616691

<https://centralesupelec.hal.science/hal-03616691v1>

Submitted on 25 Mar 2022

HAL is a multi-disciplinary open access archive for the deposit and dissemination of scientific research documents, whether they are published or not. The documents may come from teaching and research institutions in France or abroad, or from public or private research centers.

L'archive ouverte pluridisciplinaire **HAL**, est destinée au dépôt et à la diffusion de documents scientifiques de niveau recherche, publiés ou non, émanant des établissements d'enseignement et de recherche français ou étrangers, des laboratoires publics ou privés.

USE OF SENTINEL-1 TIME-SERIES FOR ARCHAEOLOGICAL STRUCTURES DETECTION

F. Michenot[§], G. Manfredi[§], R. Guinvarc'h[§] and L. Thirion-Lefevre[§]

[§]SONDRA, CentraleSupélec, Université Paris-Saclay, F-91190 Gif-sur-Yvette, France

ABSTRACT

The spatial and temporal diversity provided by Sentinel-1 SAR images is used to detect archaeological structures. The temporal mean over a year suppresses speckle without reducing spatial resolution. The combined use of the *ascending* and *descending* orbits makes it possible to highlight man-made features.

Index Terms— SAR, Sentinel-1, time-series, archaeological sites.

1. INTRODUCTION

The Copernicus program gives access to a massive amount of Earth observation data. The full utilization of the phase and intensity of SAR imagery has enabled the consolidation in the literature of some applications such as land cover changes [1, 2] and ship detection [3].

Recently, an emerging application concerns itself with using SAR imagery to detect archaeological sites or hidden ruins instead. Moore *et al.* have explored the ancient Angkor site using polarimetry and interferometry data [4]. Stewart *et al.* have used C- and L-band SAR data to detect buried archaeological structures [5]. COSMO-Sky-Med data have been used by Tapete *et al.* to monitor cultural heritage sites in Peru, Syria, Italy, and Iraq [6].

Sentinel-1 provides us regularly with new SAR images taken from two perspectives deriving from its ascending and descending orbits. This paper explains how this temporal and spatial diversity can be leveraged to assist in detecting archaeological sites obscured by a forest canopy. In detail, the technique based on the combination of the images arising from the ascending and descending orbits is presented in Section 2. Some structures of the archaeological sites of Angkor Wat and El Mirador detected with the proposed method are shown in Section 3.

2. PRINCIPLES

Sentinel-1 is a set of SAR-imaging satellites launched by the European Space Agency (ESA). The satellites are on the same heliosynchronous orbit, meaning that they will each cover the same location on the Earth at the same time of day every orbital repeat cycle (12 days). Moreover, they will actually scan

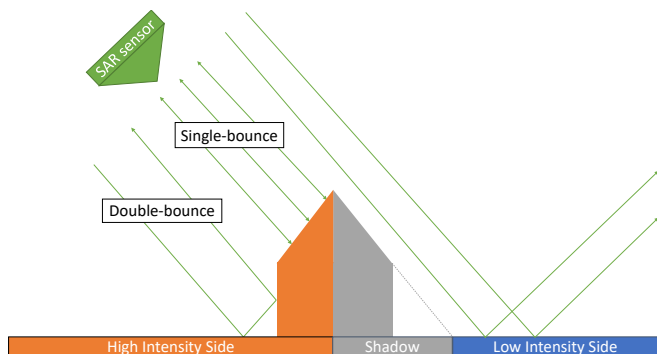


Fig. 1: Illustration of the scattering mechanisms occurring when observing a man-made structure.

places twice: once when going from the South Pole to the North Pole (*ascending*) and once when going the other way around (*descending*). These two orbital directions provide us with two perspectives over our areas of interest.

In this study, we will use Ground Range Detected (*GRD*) images. We are therefore limited to VV+VH orthorectified images with a spatial resolution of 20 m. The radiometric images are shown in Fig. 2a and Fig. 2b for the ascending and descending paths respectively.

In order to reduce the speckle without losing spatial resolution, we make use of time-series by computing the mean intensity of each pixel over the temporal axis (Fig. 3a and 3b). We arbitrarily chose to average a year of data, i.e. in general over 30 images per orbit. This is enough to counteract speckle without making computations too long. In fact - as long as buildings were not built or demolished during that period - this will actually improve the contrast between permanent (man-made structures, but also terrain features) and ephemeral (cars, forest canopy variations) targets.

This temporal mean over the (linear) pixel value is obtained as follows (for VV polarized images):

$$VV_d(x, y) = \frac{1}{N_d} \sum_{t=1}^{N_d} VV_d(x, y, t) \quad (1)$$

where N_d is the number of individual images taken from the d direction (*ascending* or *descending*) during a chosen period, $VV_d(x, y, t)$ is the intensity of the pixel located at the (x, y) spatial coordinates on the t^{th} image; $VV_d(x, y)$ provides the

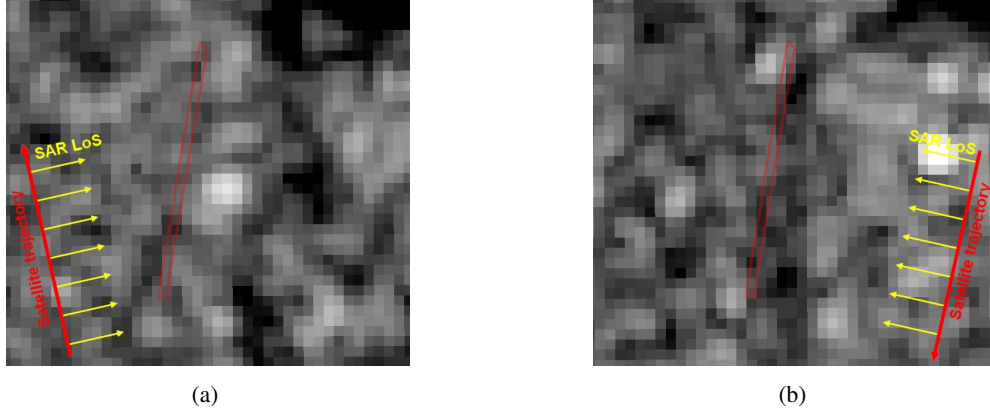


Fig. 2: SAR images of a tree-lined road near Angkor Wat, Cambodia: (a) ascending path - orbit 99, (b) descending path - orbit 91.

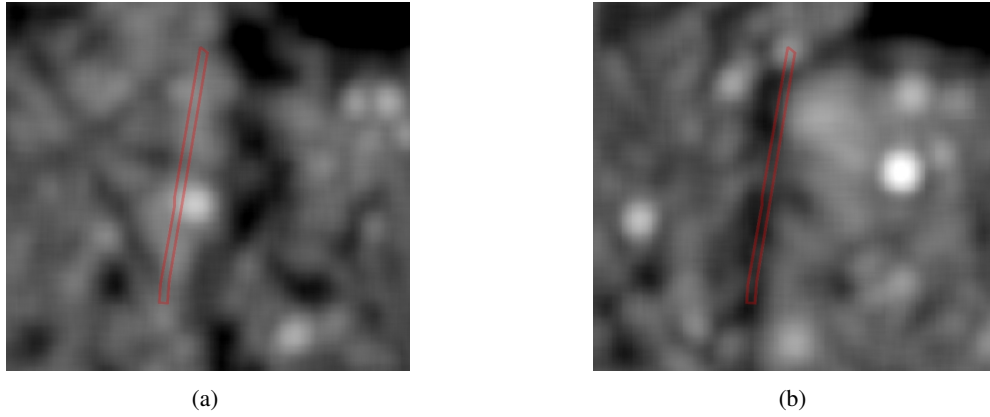


Fig. 3: Temporally-filtered SAR images of the tree-lined road: (a) ascending path - orbit 99, (b) descending path - orbit 91.

averaged intensity.

Our technique is based on the diversity of directions provided by Sentinel-1. Because the satellite is right-looking, images taken on an *ascending* orbit are viewed from the west, whereas on *descending* orbits, they are viewed from the east. Therefore, the western side of a building will have a higher reflectivity on *ascending* images than on *descending* images, and vice-versa. On the one hand, the SAR shadow cast by the building reduces the intensity on one side of it. On the other hand, single- and double-bounces that occur over the building surface increase the intensity on its other side (Fig. 1).

We exploit this by computing the difference Δ between the ascending and descending point-of-view for each pixel. When using the averaged images obtained using Eq. (1), we get the following equation (in VV polarization and dB):

$$\begin{aligned} \Delta VV(x, y) &= 10 \log_{10} \left(\frac{VV_a(x, y)}{VV_d(x, y)} \right) \\ &= VV_{a dB}(x, y) - VV_{d dB}(x, y) \end{aligned} \quad (2)$$

where a and d denote respectively the ascending and descending directions.

We display the resulting image using an RGB palette in Fig. 4b. The pixels of positive value (red) are the ones best seen from the west, those of negative value (blue) from the east, and those around zero (green) from both directions. An optical picture (4a) is provided for reference.

3. EXAMPLES OF SIGNATURES AROUND ANGKOR WAT AND EL MIRADOR

The area around the temple of Angkor Wat (Cambodia) contains a number of interesting structures whose signatures with our technique are noteworthy. The archaeological site of El Mirador, in Guatemala, was also studied.

3.1. A couple of trees

This couple of trees located near the main entrance of Angkor Wat is isolated from the rest of the forested areas (Fig. 5a). Their joint canopy has a horizontal diameter of about 20m, and the trees are at least 10m tall. They, and the SAR shadows they cast, should therefore be easily visible.

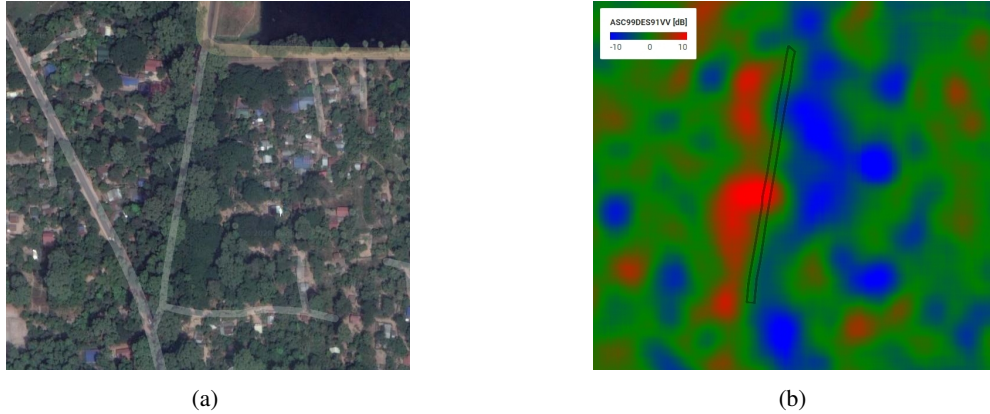


Fig. 4: A tree-lined road: (a) Optical image (© CNES/Airbus, Maxar Technologies, 2021). (b) The road as viewed when computing the difference (in dB) between the temporally-filtered ascending and descending images.

As can be seen in Fig. 5b, it is indeed the case. There is a clear east-west discrimination, along with a thin green vertical line indicating the middle of the grove.

3.2. A tree-lined road

The tree-lined road which we discussed in Section 2 provides us with a clear example closer to our application, as rows of trees do not appear naturally. The road is completely covered by the canopy (Fig. 4a). Nevertheless, it can be detected as the aligned trees create the red-blue framing seen in Fig. 4b.

We can notice, however, that the green line - framed by the red and blue areas - is not straight. Several hypotheses can be proposed to explain this effect: it can be due to the topography or the various heights or canopy densities of the trees, for instance.

3.3. El Mirador, Guatemala

The archaeological site of El Mirador, in the northern jungles of Guatemala, is composed of several ruined Mayan structures (Fig. 6a). The Leon Pyramid (northernmost marker) is completely covered by the forest and cannot be clearly observed on optical imagery. Using our technique, we can clearly tell that a structure is possibly located at this site (Fig. 6b).

The other two marked pyramids are also visible in Fig. 6b, and some smaller unmarked structures might also be distinguished (see the black arrows in Fig. 6b). The Jaguar Paw Temple is a smaller structure near the foot of the Templo Tigre Pyramid. It cannot be clearly detected.

The large red line going diagonally across the image is in the continuity of a terrain feature. However, the fact that it is straight with some right-angle branches and that it borders the structures present on the site indicates that it might in fact be a man-made structure itself, probably a wall.

4. CONCLUSIONS

This article explained how the use of time-series to reduce speckle can be joined with the computation of the difference between ascending and descending images to detect archaeological sites. This difference can highlight man-made features characterized by strong responses present in both ascending and descending directions.

This method has been demonstrated for large or tall structures within forests, using Sentinel-1 GRD products. Additionally, ruins are not the only targets detected within forests: more subtle structures like roads or walls have also been detected.

Some terrain features may also have strong signatures. They should ideally be removed.

5. REFERENCES

- [1] D. Amitrano, G. Di Martino, A. Iodice, D. Riccio, and G. Ruello, "Unsupervised rapid flood mapping using Sentinel-1 GRD SAR images," *IEEE Transactions on Geoscience and Remote Sensing*, vol. 56, no. 6, pp. 3290–3299, 2018.
- [2] S. G. Dellepiane and E. Angiati, "A new method for cross-normalization and multitemporal visualization of SAR images for the detection of flooded areas," *IEEE Transactions on Geoscience and Remote Sensing*, vol. 50, no. 7, pp. 2765–2779, 2012.
- [3] T. Taillade, L. Thirion-Lefevre, and R. Guinvarc'h, "Detecting Ephemeral Objects in SAR Time-Series Using Frozen Background-Based Change Detection," *Remote Sensing*, vol. 12, no. 11, pp. 1720, 2020.
- [4] E. Moore, T. Freeman, and S. Hensley, "Spaceborne and Airborne Radar at Angkor: Introducing New Technology

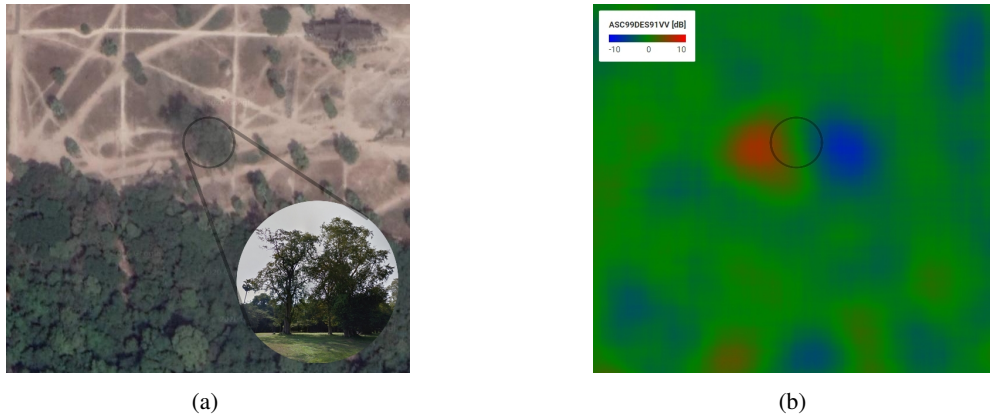


Fig. 5: Couple of trees: (a) Optical image (© CNES/Airbus, Maxar Technologies, 2021 (top-down view); © Google, 2013 (ground-level view)). (b) The trees as viewed when computing the difference (in dB) between the temporally-filtered ascending and descending images.

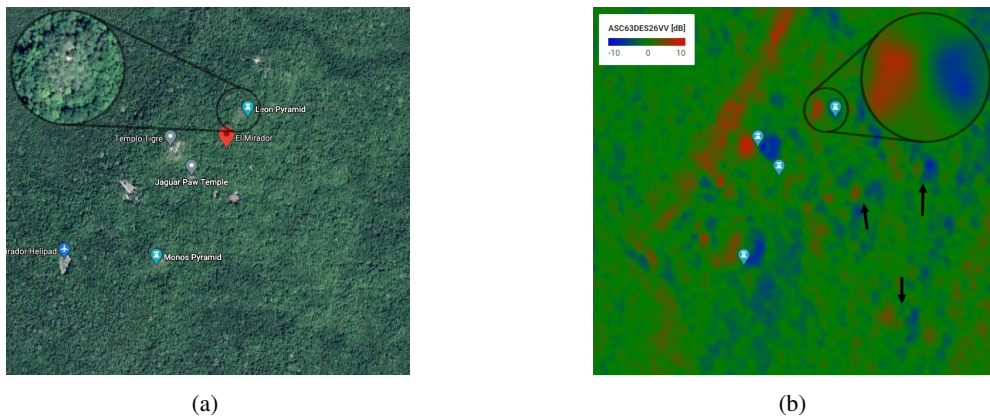


Fig. 6: El Mirador: (a) Optical image (© CNES/Airbus, Maxar Technologies, 2021 (picture); © Google, 2021 (markers)). (b) El Mirador as viewed when computing the difference (in dB) between the temporally-filtered ascending and descending images. Suspected unmarked structures are indicated by arrows.

to the Ancient Site,” in *Interdisciplinary Contributions To Archaeology*, pp. 185–216. Springer New York, 2006.

- [5] C. Stewart, R. Lasaponara, and G. Schiavon, “Multi-frequency, polarimetric SAR analysis for archaeological prospection,” *International Journal of Applied Earth Observation and Geoinformation*, vol. 28, pp. 211–219, may 2014.
- [6] D. Tapete and F. Cigna, “COSMO-SkyMed SAR for detection and monitoring of archaeological and cultural heritage sites,” *Remote Sensing*, vol. 11, no. 11, pp. 1326, 2019.